STAR Results on High Transverse Momentum, Heavy Flavor and Electromagnetic Probes

M. Calderón de la Barca Sánchez (for the STAR‡ Collaboration)
University of California, Davis
One Shields Ave
Davis, CA 95616

E-mail: mcalderon@ucdavis.edu

Abstract. We summarize here recent results from the STAR collaboration focusing on processes involving large momentum transfers. Measurements of angular correlations of di-hadrons are explored in both the pseudorapidity (η) and azimuthal (ϕ) projections. In central $Au + Au$, an elongated structure is found in the η projection which persists up to the highest measured $p_\perp$. After quantifying the particle yield in this structure and subtracting it from the near-side yield, we observe that the remainder exhibits a behavior strikingly similar to that of the near-side yield in $d + Au$. For heavy flavor production, using electron-hadron correlations in $p + p$ collisions, we obtain an estimate of the b-quark contribution to the non-photonic electrons in the $p_\perp$ region 3-6 GeV/c, and find it consistent with FONLL calculations. Together with the observed suppression of non-photonic electrons in $Au + Au$, this strongly suggests suppression of b-quark production in $Au + Au$ collisions. We discuss results on the mid-rapidity Υ cross-section in $p + p$collisions. Finally, we present a proof-of-principle measurement of photon-hadron ($\gamma - h$) correlations in $p + p$ collisions, paving the way for the tomographic study of the matter produced in central $Au + Au$ via γ-jet measurements.
PACS numbers: 25.75.-q, 25.75.Nq, 12.38.Mh, 25.75.Gz, 13.20.Gd

1. Introduction

Without question, some of the most exciting results that have been observed in the study of relativistic heavy-ion collisions in the RHIC era have been in the area of processes with large momentum transfers. All collaborations observed evidence of large *final state* suppression of the inclusive yield of charged hadrons at high transverse momenta ($p_\perp$) in central $Au + Au$ collisions [1–4], by as much as a factor of 5. The study of azimuthal correlations demonstrated that the suppression mainly affects hadrons found in the away-side of the leading particle in the event [3, 5], and that this suppression was not present in $d + Au$ collisions. The consensus reached around these observations was that RHIC produces extremely dense matter ($\sim$ 50 times higher than ground-state nuclei), and the suppression patterns were the result of induced gluon radiation as fast partons traversed this dense medium [6–9].

‡ Full collaboration list found in Appendix

The focus for the last two years of RHIC research in this area has been the quantitative determination of the properties of the produced matter, *e.g.* its density, temperature and viscosity. Reliable estimations of these is the current challenge of the heavy-ion program. To determine the density quantitatively, the inclusive suppression was the first observable used to compare to theory, but in essentially all theoretical descriptions the level of suppression in the range $\lesssim$ 20GeV shows a saturation with increasing density, (see *e.g.* [10, 11]), so further information is needed to constrain the models. Several measurements can provide further clues. First, to complete a systematic study of di-hadron correlations. Second, to use heavy quarks as probes, given that they are expected to couple less strongly to the medium. Finally, to measure photon-jet correlations to vary the geometry bias compared to di-hadron correlations. Together, the study of di-hadron correlations, heavy quarks and γ-jet measurements should provide sufficient sensitivity to quantitatively determine the density of the medium. We discuss now the results relevant to these probes presented at this conference by STAR. The summary of results for identified spectra at lower momenta, strangeness, azimuthal anisotropy and three-particle correlations is presented in Ref. [12].

2. Di-hadron Correlations

The interest in a systematic study of di-hadron correlations stems from the need to better understand the interaction of fast partons with the bulk of the produced medium. It is established that the away-side particles are strongly modified by the dense matter, leading to suppression of the yields [5]. The observation of broad away-side correlations at low $p_\perp$ [13] make clear that lowering the $p_\perp$ is also necessary to fully understand the system. Previous results on di-hadron $\eta - \phi$ correlations used untriggered particles with $p_\perp < 2$ GeV/c [20]. At intermediate $p_\perp$, the observation of dip-hump structures in the away-side correlation functions [15, 16] have generated much interest and speculation as to the nature of the medium response to a fast parton. At high $p_\perp$, clear di-jet signals are observed [14] and the use of di-hadron fragmentation functions has been proposed as an additional tool for quantitative comparison to energy-loss phenomenology. We now aim to map the angular correlation panorama, extending the $\eta - \phi$ measurements using triggered hadrons with $p_\perp > 2$ GeV/c [17], forward-to- mid-rapidity ϕ correlations, [18], and extending previous ϕ correlation and di-hadron fragmentation measurements to study the ${p_\perp}^{\rm trig}$ systematics [19].

We first summarize results from the $\Delta\phi - \Delta\eta$ correlation analysis at mid-rapidity ($|\eta| < 1$). At low-$p_\perp$, there are already quantitative measurements [20] of the number and $p_\perp$ correlation in $\eta - \phi$ which show a ϕ elongation of the 2-D number correlation in $p+p$ collisions, and an η elongation (both in number and $p_\perp$ correlations) in $Au+Au$ for $p_\perp < 2$ GeV/c. The results presented here extend the reach to the region $2 < {p_\perp}^{\rm assoc} < 4$ GeV and $3 < {p_\perp}^{\rm trig} < 12$ GeV, using the trigger-associated technique [5]. Figure 1(left), presents the $\Delta\eta - \Delta\phi$ correlation, choosing tracks with ${p_\perp}^{\rm assoc} > 2$ GeVand $3 < {p_\perp}^{\rm trig} < 4$ GeV in the 10% most central $Au+Au$ events.

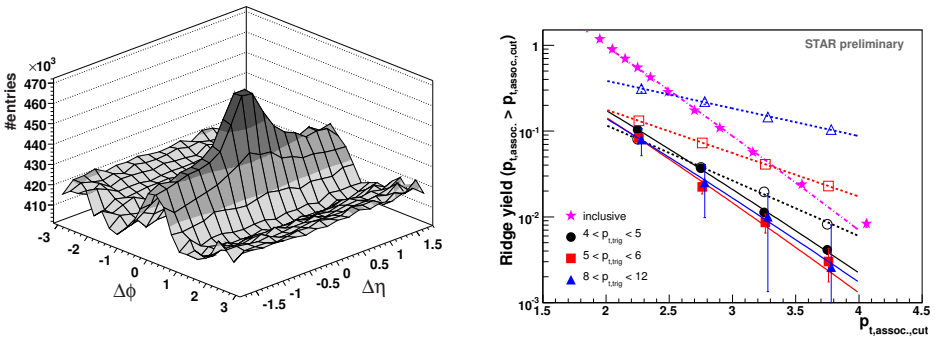

Figure 1. Left: $\Delta\eta - \Delta\phi$ correlation in $Au + Au$ collisions, showing an elongation along the pseudorapidity-difference direction. We separate the correlation into two components which we label "jet" and "ridge" (see text for details) and study the yields in each component. Right: Invariant yields *vs.*$p_\perp{}^{\rm assoc}$ for the "jet" (dashed lines, open symbols) and "ridge" components (solid lines, filled symbols). The different symbols are for various choices of $p_\perp{}^{\rm trig}$.

We note the v_2 elliptic flow modulation in the azimuth-difference axis, and for the region near $\Delta\phi = 0$ an η correlation that is present throughout the η acceptance of the STAR TPC. The correlation shows a maximum in the region near $\Delta\eta = \Delta\phi = 0$. To quantitatively study the yields as a function of centrality and of the $p_\perp{}^{\rm assoc}$ and $p_\perp{}^{\rm trig}$ kinematics, we employed the following ansatz. We divide the correlation yield into two components. The first component is constructed to resemble a jet-like correlation. We do this in three different ways. One is to choose two disconnected regions in $\Delta\eta$, a region away from the maximum ($0.7 < |\Delta\eta| < 1.4$) and a region near the maximum ($|\Delta\eta| \leq 0.7$) (see Ref. [17, 21] for more details and examples). Subtracting the former from the latter, we obtain a component that we label the "jet"-like correlation $\Delta\eta(J)$, borrowing from the picture of a QCD jet fragmenting into hadrons. The yield remainder in the region $|\Delta\phi| < 0.7$ we label the "ridge"-like correlation, due to the obvious shape. While this decomposition is instructive to produce quantitative measurements of the yields *vs.* centrality and *vs.* the $p_\perp$ kinematics, it should be noted that this does not imply that the ridge-like correlation is unrelated to jet-fragmentation phenomena.

Once we use the decomposition into the "jet" (J) and the "ridge" (R), we can study the yields. We find the total yield ($J + R$) increases linearly as a function of $N_{\rm part}$, but after removing the ridge yield R, the remainder J yield is independent of centrality (see [17]). Focusing on central collisions, Fig.1(right) shows the yield in varying bins of $p_\perp{}^{\rm assoc}$ for windows of $p_\perp{}^{\rm trig}$ for the J component (open symbols) and the R component (filled symbols). We fit an exponential to each resulting $p_\perp{}^{\rm assoc}$ spectrum; dashed lines for the J spectra and solid lines for the R spectra. For reference, the inclusive spectrum is shown (stars). We observe that the R spectra have similar slopes to the inclusive spectra, and the overall shape and yields are independent of $p_\perp{}^{\rm trig}$ within our uncertainties. In contrast, the J spectra are all harder than the inclusive, and a clear correlation is seen between the slope and yield of the J spectrum and the choice of $p_\perp{}^{\rm trig}$.

Studies on $\Delta\phi$ correlations can now benefit from the knowledge of this elongated $\Delta\eta$ structure in the near-side. Figure 2 shows the result of applying the $J + R$ ansatz to the near-side di-hadron fragmentation functions *vs.* $z_\perp \equiv {p_\perp}^{\rm assoc}/{p_\perp}^{\rm trig}$.

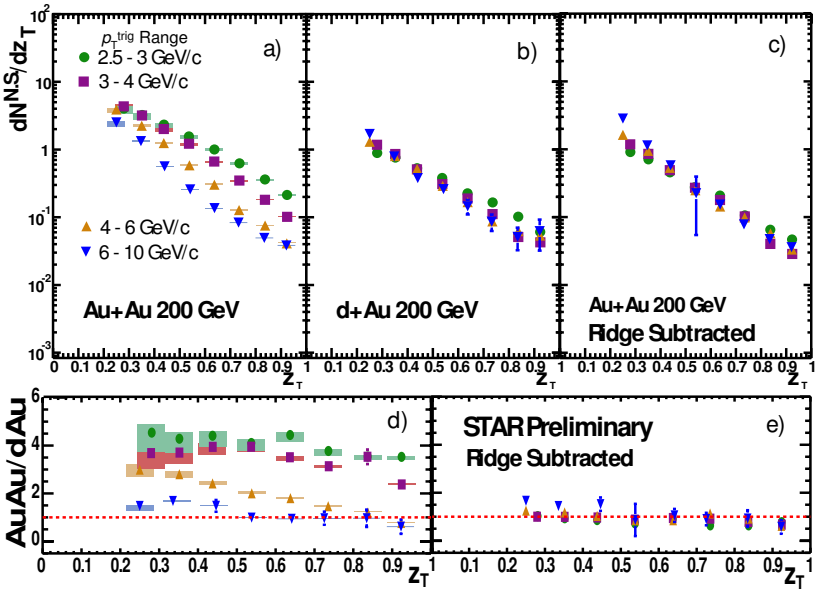

Figure 2. $Au + Au$ (a) and $d + Au$ (b) $z_\perp$ distributions. The ratio of $Au + Au$ to $d + Au$ is shown in (d). $Au + Au$ after subtraction of the "ridge" yield is shown in (c), and its ratio to $d + Au$ is shown in (e).

Figure 2a) shows the $Au + Au$ $p_\perp$-triggered di-hadron fragmentation functions *vs.* $z_\perp$ for various windows in ${p_\perp}^{\rm trig}$. The top-middle panel shows the same study for $d + Au$, where the $z_\perp$ dependence of the $d + Au$ data has a similar shape for all choices of ${p_\perp}^{\rm trig}$. Panel d) shows the ratio of the $z_\perp$ spectra in $Au + Au$ to that in $d + Au$. All $z_\perp$ spectra have similar slopes in $Au + Au$ compared to $d + Au$, but the yields are larger in $Au + Au$ for lower ${p_\perp}^{\rm trig}$. Removing the R component, as shown in Fig. 2c), we find the remaining particles behave just like $d + Au$: Fig. 2e) shows the ratio of the R removed $z_\perp$ spectra in $Au + Au$ to the $d + Au$ spectrum, seen to be close to unity within our uncertainties for all ${p_\perp}^{\rm trig}$ windows. This is suggestive that the J component might be indicative of vacuum fragmentation after energy loss. Together with the quantitative study of the low-$p_\perp$ number and $p_\perp$ correlations, these measurements should provide a reference against which models attempting to constrain the density of the medium can be compared.

3. Heavy Flavor

3.1. e-h Correlations

The trigger-associated correlation technique has been extended to use electron triggers. Experimentally, measurements of the non-photonic electron spectra are used as a proxy for heavy quarks. These show a rather large amount of suppression [22] in $Au + Au$, much larger than initial calculations of heavy-quark energy loss predicted [23]. The mechanism of energy loss for heavy quarks was reassessed, with the conclusion that collisional energy loss is important [24].

Nevertheless, the calculations were still not able to reproduce the level of suppression measured for the non-photonic electrons. Since the measurement is sensitive to the sum of the c and b quark contributions, it was also noted that if the b-quark contribution was modified (and in the extreme case, *ignored*) the calculations were consistent with the measurement. Therefore, an urgent need arose for disentangling the relative contributions of c and b quarks to resolve the ambiguity. We present here the first results from a method to extract the b contribution to the non-photonic electrons via the analysis of $e-h$ correlations in $p+p$ collisions.

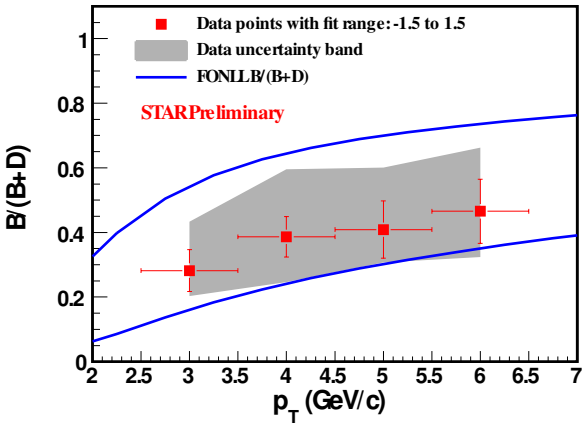

Figure 3. B-meson contribution to the non-photonic electrons extracted from a fit to $e-h$ azimuthal correlations in $p+p$ collisions.

The method exploits the correlation between the electron and hadron that originate from the semi-leptonic decay of a heavy-quark. The larger mass of the B meson results in a larger energy given to the decay products, which results in a broader near-side $e-h$ correlation compared to that resulting from the semi-leptonic decay of a D meson. We have simulated the resulting $e-h$ correlation shapes using PYTHIA, which introduces a model-dependence into the method. The model-dependence is small however: varying the underlying fragmentation functions we find no significant modification of the B and D correlation shape. In other words, the correlation shapes are to first order sensitive only to the kinematics of the decay given the meson masses (a much tighter constraint). The details of the analysis (background subtraction, fitting procedure and $B/(B+D)$ ratio extraction) are in Ref. [25]. Figure 3 shows the resulting $B/(B+D)$ ratio from this analysis (filled squares). The error bars are statistical, and the shaded band is the systematic uncertainty (mainly from photonic-background reconstruction efficiency). The two lines in the figure are from FONLL calculations, showing the bounds of the theoretical uncertainties (mass and renormalization scale). The data from this measurement are consistent with the FONLL calculations. This has important implications for the $Au+Au$ data. Since model calculations attempting to describe the non-photonic electron suppression in $Au+Au$ were not able to reproduce the large amount of suppression, a better agreement could be arrived at assuming the B contribution only starts to appear at $\sim$ 10 GeV/c. The data in Fig. 3 disallows such solution, and one is left with the conclusion that to explain the data it is necessary to suppress the B mesons in central $Au+Au$ at RHIC. A possible mechanism for B suppression discussed in Ref. [26] invokes collisional dissociation of the B mesons.

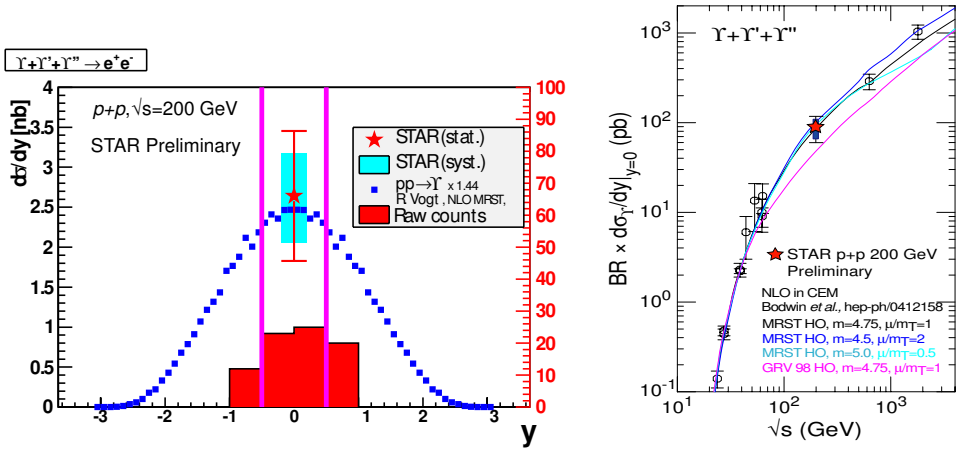

Figure 4. Left: Υ cross section ((1s+2s+3s), filled star) measured in $|y| < 0.5$ (see left abscissa for scale) compared to NLO calculations. The raw yield *vs.* y is shown as the filled histogram (see right abscissa for scale). Right: Comparison of the measured cross section to world data and NLO calculations. See text for details.

3.2. Υ *Production*

During 2006, several analyses benefited from the completion of the STAR EMC ($|\eta| < 1$ and $0 < \phi < 2\pi$). One is a measurement of the Υ production at mid-rapidity. The larger coverage of the calorimeter improves the Υ acceptance in STAR by a factor of 4 over the coverage during the 2004 run. During the 2006 $p+p$ run, we sampled an integrated luminosity of $\mathcal{L} = 9$ pb^{-1}. Two main trigger settings were used during the running period; we analyzed and obtained full corrections for one of these. Figure 4(left) shows the measurement of the Υ(1s+2s+3s) cross section $d\sigma/dy|_{y=0}$. The filled histogram shows the background-subtracted counts in the Υ mass region to illustrate the acceptance. The left abscissa shows the $d\sigma/dy$ scale and the right abscissa shows the scale for the raw-count histogram. The error bars in the cross section measurement are the statistical error and the shaded rectangle is the systematic uncertainty. The low cross section of the Υ at RHIC makes this a luminosity limited measurement. We compare the datum point to a NLO calculation of the Υ(1s) cross section scaled by 1.44 (based on CDF [27]) to account for the excited states. Figure 4(right) shows the the world data on Υ production as a function of $\sqrt{s}$, compared to NLO calculations. The NLO calculation is consistent with our measurement within our uncertainties. Future measurements of Υ production in $Au + Au$ will yield additional clues as to the temperature of the produced matter.

4. $\gamma - h$ Correlations

Finally, we present results from the analysis of photon-hadron ($\gamma - h$) correlations in $p+p$ collisions. This analysis has also benefited from the increased coverage of the calorimeter. Compared to two-particle correlations using di-hadrons, $\gamma - h$

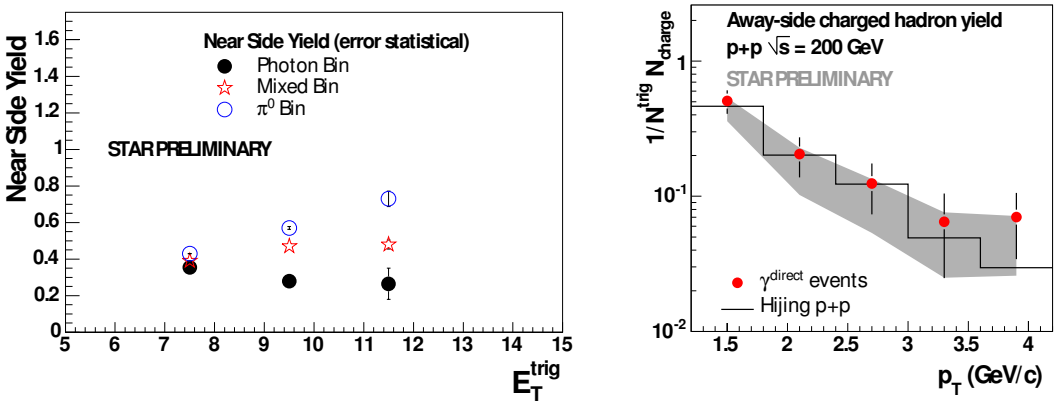

Figure 5. Left: Integrated yield of the near-side $\Delta\phi$ correlation in $p+p$ collisions for the π^0-enriched (open circles), mixed (open stars), and γ-enriched (filled circles) samples *vs.* $E_\perp$. Right: For the γ-enriched sample, the measured away-side yield of charged hadrons (circles) is compared to HIJING simulations selecting events with direct γ production.

measurements in $Au+Au$ hold the promise to essentially remove the surface bias that complicates the interpretation and model comparison of the correlations. Since the photon will not suffer the effects of energy loss it can be used as a reference for the momentum transfer of the partonic hard process.

In the analysis of $\gamma - h$ correlations, the dominant source of background to the measurement of direct photons is π^0 contamination. The EMC shower maximum detector (SMD) is employed as a discriminator between direct γ's and π^0's (for details, see Ref. [28]). The SMD showers can be used to select showers with π^0-like shape, γ-like shape, or somewhere in between. The tell-tale signature of a direct γ is that it should have no associated hadrons near it in $\eta - \phi$. Figure 5(left) shows the near-side yields of the π^0-enriched (open circles), mixed (open stars), and γ-enriched (filled circles) samples *vs.* $E_\perp$. The γ-enriched data show a decrease of the yield at high $E_\perp$, consistent with the expected behavior for γ-jet events. For this sample, the away-side yield is compared to γ-jet simulations using HIJING in Fig. 5(right). The observed $p_\perp$ spectrum of the away side yields is consistent with the calculations within our experimental uncertainty, an encouraging development for future tomographic explorations of the medium using high-$E_\perp$ photons.

5. Conclusions

We have measured di-hadron correlations in a large fraction of the available kinematics at RHIC energies. We presented in this conference results on $\Delta\eta - \Delta\phi$ correlations at intermediate- to high-$p_\perp$. Using a simple ansatz to isolate the yield in the jet-like near-side region and subtracting it from the total to quantify the yield in the "ridge" region, we observe that the near-side jet-like peak shows compatibility with vacuum

fragmentation behavior. Our hope is that with the quantitative measurements of the correlations from low, intermediate and high-$p_\perp$ will be less "fragile" than single inclusive spectra, and this robustness can provide tighter constraints on the estimations of the density. The analysis of $e-h$ correlations has yielded the first estimate of the B contribution to the non-photonic electrons in $p+p$; we find it consistent with FONLL calculations. Together with the measured suppression of the non-photonic electron inclusive spectrum, the corollary of this observation is that there must be B suppression at RHIC in $Au+Au$. We presented first $p+p$ results from two luminosity-hungry measurements: the Υ cross section and the $\gamma-h$ correlation. A larger integrated luminosity in future runs and RHIC II should allow a measurement of the Υ (2s)/(1s) and (3s)/(1s) ratios: perhaps one of the most direct ways to connect experimental data to a temperature calculated from lattice QCD. The $\gamma-h$ measurement allows experimentalists to vary the surface bias that exists in measurements relying on particles which suffer energy loss, so it can be one of the ultimate probes of the medium density. Having performed the proof-of-principle measurements, we now eagerly await a chance to take the data to complete these programs.

6. References

[1] B. B. Back *et al.* [PHOBOS Collaboration], Phys. Rev. Lett. **91**, 072302 (2003)
[2] S. S. Adler *et al.* [PHENIX Collaboration], Phys. Rev. Lett. **91**, 072303 (2003)
[3] J. Adams *et al.* [STAR Collaboration], Phys. Rev. Lett. **91**, 072304 (2003)
[4] I. Arsene *et al.* [BRAHMS Collaboration], Phys. Rev. Lett. **91**, 072305 (2003)
[5] C. Adler *et al.* [STAR Collaboration], Phys. Rev. Lett. **90**, 082302 (2003)
[6] I. Arsene *et al.* [BRAHMS Collaboration], Nucl. Phys. A **757**, 1 (2005)
[7] B. B. Back *et al.*, Nucl. Phys. A **757**, 28 (2005)
[8] J. Adams *et al.* [STAR Collaboration], Nucl. Phys. A **757**, 102 (2005)
[9] K. Adcox *et al.* [PHENIX Collaboration], Nucl. Phys. A **757**, 184 (2005)
[10] A. Dainese, C. Loizides and G. Paic, Eur. Phys. J. C **38**, 461 (2005)
[11] K. J. Eskola, H. Honkanen, C. A. Salgado and U. A. Wiedemann, Nucl. Phys. A **747**, 511 (2005)
[12] L. J. Ruan, *et al.* [STAR Collaboration], these proceedings.
[13] J. Adams *et al.* [STAR Collaboration], Phys. Rev. Lett. **95**, 152301 (2005)
[14] J. Adams *et al.* [STAR Collaboration], Phys. Rev. Lett. **97**, 162301 (2006)
[15] S. S. Adler *et al.* [PHENIX Collaboration], Phys. Rev. Lett. **97**, 052301 (2006)
[16] J. G. Ulery *et al.* [STAR Collaboration], Nucl. Phys. A **774**, 581 (2006)
[17] J. Putschke *et al.* [STAR Collaboration], these proceedings.
[18] L. Molnar *et al.* [STAR Collaboration], these proceedings.
[19] M. J. Horner *et al.* [STAR Collaboration], these proceedings.
[20] J. Adams *et al.* [STAR Collaboration], Phys. Rev. C **73**, 064907 (2006)
[21] J. Bielcikova *et al.* [STAR Collaboration], these proceedings.
[22] B. I. Abelev *et al.* [STAR Collaboration], arXiv:nucl-ex/0607012.
[23] Y. L. Dokshitzer and D. E. Kharzeev, Phys. Lett. B **519**, 199 (2001) [arXiv:hep-ph/0106202].
[24] M. Djordjevic, Phys. Rev. C **74**, 064907 (2006) [arXiv:nucl-th/0603066].
[25] X. Y. Lin *et al.* [STAR Collaboration], these proceedings.
[26] A. Adil and I. Vitev, arXiv:hep-ph/0611109.
[27] F. Abe *et al.* [CDF Collaboration], Phys. Rev. Lett. **75**, 4358 (1995).
[28] S. Chattopadhyay *et al.* [STAR Collaboration], these proceedings.